Methylene blue-encapsulated liposomal biosensor for electrochemical detection of sphingomyelinase enzyme

Methylene blue-encapsulated liposomal biosensor for electrochemical detection of sphingomyelinase enzyme

Ankan Dutta Chowdhury[a] and Enoch Y. Park[a,b,*]

[a] *Research Institute of Green Science and Technology, Shizuoka University, 836 Ohya Suruga-ku, Shizuoka 422-8529, Japan*

[b] *Department of Bioscience, Graduate School of Science and Technology, Shizuoka University, 836 Ohya Suruga-ku, Shizuoka 422-8529, Japan*

[*]Corresponding Author at Research Institute of Green Science and Technology, Shizuoka University, 836 Ohya Suruga-ku, Shizuoka 422-8529, Japan.

E-mail addresses: park.enoch@shizuoka.ac.jp (E.Y. Park), ankan.dutta.chowdhury@shizuoka.ac.jp (A.D. Chowdhury).

ABSTRACT

Sphingomyelinase (SMEnzyme) converts sphingomyelin into ceramide, modulating membrane properties and signal transduction which inactivates mutations and causes Niemann–Pick disease. Real time monitoring of SMEnzyme is also crucial as an important biomarker for several other diseases like atherosclerosis, multiple sclerosis, and HIV. In this study, we present an electrochemical method to detect SMEnzyme concentration that is more sensitive and much faster than currently available commercial assays. For detection and the amplification of the SMEnzyme signal, methylene blue (MB)-encapsulated sphingomyelin (SM)-based liposome with 50 % cholesterol was synthesized via sonication method. Then the target SMEnzyme causes the free release of the MB from the MB-liposome formulation which can be detected on GCE||Au-PAni/N,S-GQDs electrode, prepared via interfacial polymerization and then self-assembly approach. The change of SM to gel state bilayer with increasing concentration of ceramide accounts for the observed increase in membrane permeability and consequent release of encapsulated MB as the redox indicator for electrochemical Differential Pulse Voltammetric (DPV) analysis. To get the optimum capture through π–π stacking interaction of the released MB on the Au-PAni/N,S-GQDs nanocomposites, which has been used as working electrode. Minimal cross-reactivity with similar phospholipase and proteins confirms the stable and non-leaky MB-liposome platform with low background signal and high specificity toward SMEnzyme. Additionally, the applicability of the proposed sensor has successfully verified in three possible sources of human serum, plasma and cell supernatant without compromising its performance. Taken together, the simplicity, rapid response time and high sensitivity of this present method offer huge potential in point-of-care diagnostics of SMEnzyme detection.

Keywords: Differential pulse voltammetric, Electrochemical detection, Liposome, Methylene blue, Sphingomyelin, Sphingomyelinase

1. Introduction

Sphingomyelinase (SMEnzyme) is an important enzyme found in lysosomes and in the extracellular space where it catalyzes sphingomyelin (SM) which is an important class of phospholipids, constituting 2 – 15 % of the total phospholipid content of mammalian tissues [1, 2]. SMs and other sphingolipids are widely reported to induce structural rigidity in cell membranes [3]. However, recently, its function has been explored more than a structural one [4]. Lack of SM activity leads to Niemann–Pick disease [5], atherosclerosis [3], depression [6], multiple sclerosis [7] and human immunodeficiency virus (HIV) infection [6]. Upon activation by different stimuli such as cytokines, irradiation, or serum deprivation, SM generates antiproliferative ceramides from the membrane constituent sphingomyelin and has hence been attributed a crucial role in cell fate [8]. On the other hand, up-regulated SMEnzyme activity provides a reliable biomarker target for improved diagnostic and prognostic tools, which could significantly improve patient outcome [9]. Therefore, the development of a rapid and sensitive technique to detect the SMEnzyme is highly desirable in point-of-care sensors for disease diagnosis and treatment to ensure the health safety. However, current SMEnzyme activity relies only on complicated multistep enzymatic reactions which require expensive equipment or usage of radioactive markers or non-natural substrates [7, 10-12]. It makes the detection expensive, low sensitive, time consuming and hence less effective for practical application.

Several SMEnzyme screening assays have been reported so far including fluorometric [8, 10], colorimetric [9, 13] and radioactive assays [12]. These assays are mainly based on either artificial substrates or radiolabeled substrates which have strong limitation for application. To achieve a sensible method to identify the quantity of SMEnzyme in different compositions, liposome aggregation and phosphate quantification-based assays have been emerged as most successful [9, 14, 15]. Recently, A FRET probe-based biosensor has been developed that enable the in situ non destructive detection of enzymatic cleavage of SMEnzyme by

fluorescence imaging [8]. However, these assays are mostly reliable over the enzyme activities of 1 U mL^{-1} which are less sensitive than the required quantity of mU range. To obtain high sensitivity, few reports showed the liposome conjugated natural and synthetic lipids to release their cargo in the presence of a target protein, causing a colorimetric or fluorometric responses [16, 17]. Release of encapsulated contents from the SM based liposomes can also be triggered by SMEnzyme and some analyzing factors inside the liposomes can reach to high sensitivity. Mixtures of SM with cholesterol and phospholipids such as phosphatidylcholines (PC) and phosphatidylethanolamines (PE) have also been tested to be substantially more active toward SMEnzyme than pure SM [14]. However, PC and PE-containing liposomes are failed to obtain satisfactory selectivity since these phospholipids shows similar activity towards other phospholipases. So, instead of altering the liposomal structure, change of analyzing probe inside liposomes can be a good alternative to achieve the desired sensitivity without compromising the selectivity. In this regard, an electrochemically active redox probe can be a suitable option due to its ability of detection in very low concentration of analyte.

The continuous development of novel nanomaterials and nanotechnology in recent science offers new horizons for electrochemical detection which can be used for high sensitive sensing outputs [18-21]. Methylene blue (MB), belongs to the phenothiazine family, is a well-known redox probe for the use of several electrochemical studies, especially for the Differential Pulse Voltammetric (DPV) process [22, 23]. Encouraged by our previous reports on DPV analysis, in this study, self-assembled SM liposomes-encapsulated with MB (MB-liposome) has been synthesized which can be served as a potential nanoprobe for the SMEnzyme detection. According to our hypothesis, after perturbation of SM-liposome, triggering by SMEnzyme, the released MB can be detected by the DPV process (Scheme 1). To get the maximum response from the released MB, a highly electroactive Au-PAni/N,S-GQD nanocomposite-coated glassy carbon (GC) has been used as working electrode. To synthesize the Au-PAni/N,S-GQD

nanocomposite, the nitrogen-, sulphur-co-doped graphene quantum dots (N,S-GQDs) and gold-embedded polyaniline nanowires (Au-PAni) was prepared via hydrothermal method and interfacial polymerization [24], respectively and then self-assembly approach [25]. Due to the long-term stability and nanodimensional structure, polyaniline chain can offer easy influence on the interactions between the matrix and embedded Au nanoparticles [26] whereas the as synthesized gold nanoparticles (AuNPs) with well-defined and controlled shape become a promising material to capture the thiolated N,S-GQDs via soft acid-soft base-interaction [27]. Additionally, the graphitic structure of N,S-GQDs has the most promising exposed surface to capture maximum amount of released MB from the MB-liposome [28, 29]. According to the previous research, for the N,S-GQDs, the chemically bonded nitrogen atom could drastically enhance the electrochemical properties by altering the electronic characteristics whereas the sulphur can increases the number of anchoring sites for the adsorption towards AuNPs [30]. Therefore, the Au-PAni/N,S-GQD nanocomposites has used as an excellent electroactive electrode in DPV for capturing the MB whose concentration showed the indirect quantification of the target SMEnzyme. Optimizing conditions for MB-liposome formulation, the SMEnzyme detection are investigated thoroughly, even in real matrices of human plasma, serum and cell culture supernatant instead of PBS. Selective nature of the sensor was also investigated and meets the demands of its potential usage for real application.

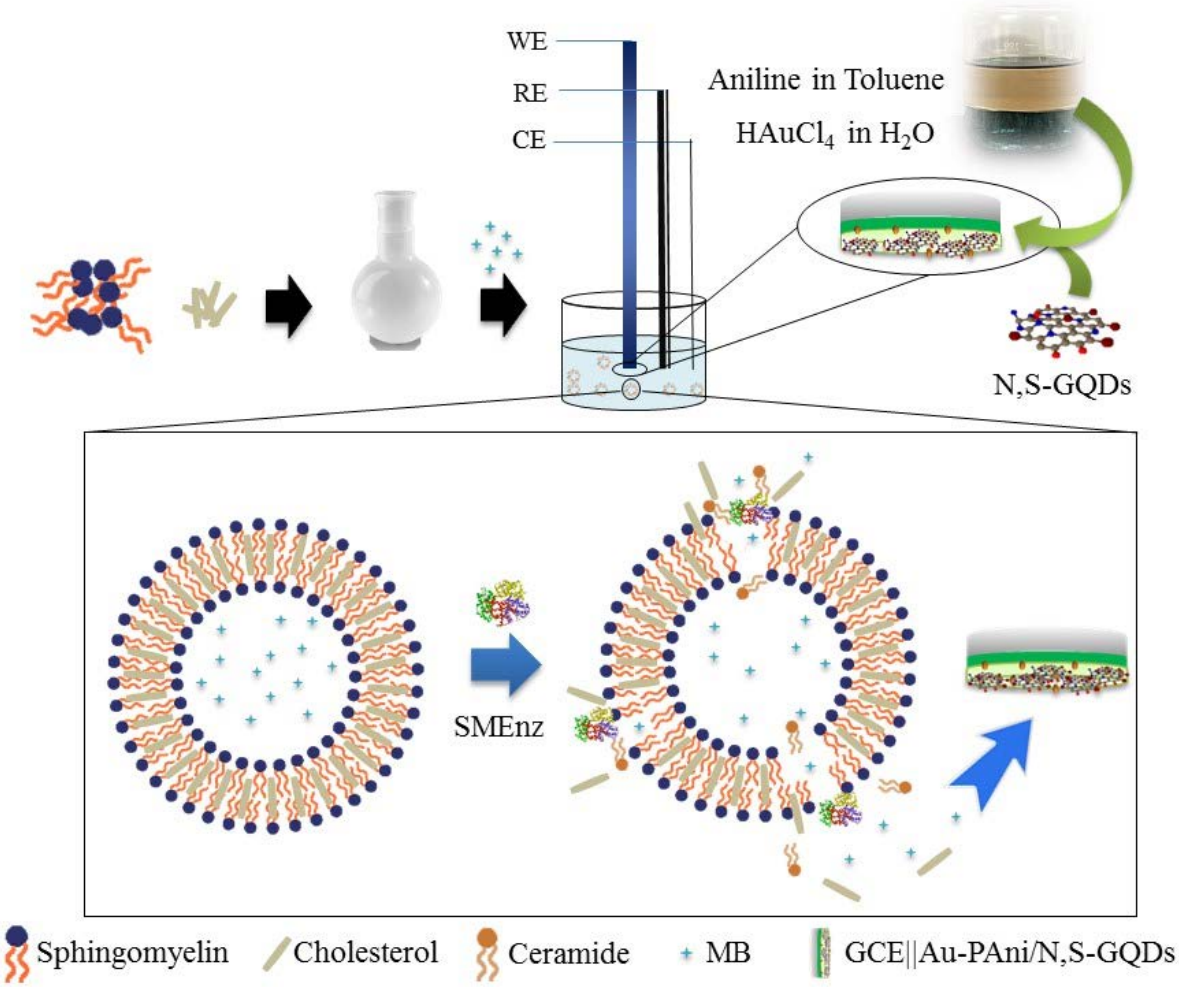

Scheme 1. Synthesis of methylene blue-encapsulated sphingomyelin liposome (MB-liposome) and its application in DPV metric based SMEnzyme detection using GCE||Au-PAni/N,S-GQD as working electrode.

2. Materials and methods

2.1. Chemicals

Citric acid, Sodium acetate and acetone were purchased from Wako Pure Chemical Ind. Ltd. (Osaka, Japan). Methylene blue, cholesterol, $HAuCl_4$, toluene, aniline, thiourea, citric acid, 1-ethyl-3-(3-dimethylaminopropyl) carbodiimide hydrochloride (EDC), N-hydroxy

succinimide (NHS), bovine serum albumin, lysozyme, phospholipase A, Triton X, human serum and human plasma were purchased from Sigma-Aldrich (St Louis, USA). Sphingomyelin and Sphingomyelinase enzyme were purchased from Avanti Polar Lipids, Alabaster, AL, USA). All aqueous solutions were prepared using high-purity deionized (DI) water (>18 MΩ cm^{-1}).

2.2. Synthesis of N, S-GQDs

The nitrogen and sulphur doped graphene quantum dots (N,S-GQDs) were prepared by standard hydrothermal method with thiourea to citric acid [30]. In brief, 0.23 g citric acid and 0.23 g thiourea were dissolved into 5 mL of deionized water and then transferred into a 20-mL of Teflon lined stainless steel autoclave tube. Then, the solution was heated up to 160 °C for 4 h to obtain the brown suspension of N,S-GQDs. It was then added into ethanol solution and centrifuged at 5000 × g for 5 min to remove the excess reagents. To obtain uniform size for further purification, the as prepared N,S-GQDs was dialyzed with 1 kDa dialysis bag for 8 h.

2.3. Synthesis of Au-PAni nanocomposites via interfacial polymerization

Au-PAni was synthesized by interfacial polymerization method, as described in our previous studies [31]. In brief, 3 mM of $HAuCl_4$ in 0.1 M HCl aqueous solution was slowly poured into 0.5 M of aniline monomer in toluene as an organic phase to initiate interfacial polymerization process. Au-PAni nanotube was slowly formed in the interface of these two layers as the solution color becomes dark green within several minutes. Then the synthesized solution was centrifuged at 5500 × g in room temperature and re-dispersed using ultrapure water for purification.

2.4. Preparation of Au-PAni/N,S-GQD-coated GCE working electrode

The as synthesized Au-PAni nanocomposites was physically mixed with excess amount of N,S-GQD and stirred overnight to prepare the Au-PAni/N,S-GQD nanocomposites. Then,

the nanocomposites were purified from the excess amount of N,S-GQDs by dialysis bag of 3 kDa for 16 h. Finally, 10 µL of the Au-PAni/N,S-GQD solution was drop-casted on the clean surface of GCE and dried under air.

2.5. Preparation of MB-liposome

Sphingomyelin (SM) and cholesterol were dissolved in a ratio of 50:50 in the solution of 1:1 methanol and chloroform, at 10 mg mL^{-1} concentrations [9]. In case of different ratios of SM:Cholesterol, solutions of were mixed in ratios of 70:30, 50:50 and 30:70 and aliquoted into 5-mL round bottom glass tubes, with a final concentration of 2 mg. Solvents were evaporated using a stream of 99.9 % nitrogen gas to give a homogeneous lipid film through the glass surface and then stored sealed in -20°C. For hydration, MB solutions of 0.1, 1, 5 and 10 mM were prepared by dilution method in PBS. The SM lipid film was hydrated with 1 mL of these MB solutions for 30 min and agitated on a vortex shaker until the lipid film had fully detached from the glass vial walls to form a homogeneous lipid suspension. To get the monodisperse unilamellar 100 nm MB-liposomes, the lipid suspension was extruded at least 5 times through a 100 nm pore sized polycarbonate membrane (Merck, Carrigtwohill, Ireland) using a micro injection.

2.6. Characterizations

The transmission electron microscopy (TEM) image for nanocomposites and liposome was taken by JEOL TEM (JEOL, Tokyo, Japan). In case of high magnified images, samples were examined with a HR-TEM (1400JEM-2100F at 200 kV, JEOL, Tokyo, Japan). Powder X-ray diffraction (PXRD) analysis was carried out using a Rint Ultima XRD (Rigaku Co., Tokyo, Japan) with a Ni filter and a Cu-Kα source. Data were collected over 2theta = 5–90º at a scan rate of 0.01º/step and 10s/point. Dynamic light scattering (DLS) measurements were performed using a Zetasizer Nano series (Malvern Inst. Ltd., Malvern, UK). UV-Vis absorption

and fluorescence emission measurements were carried out using a filter-based multimode microplate reader (Infinite F500; TECAN, Ltd, Männedorf, Switzerland). Electrochemical DPV was carried out on a SP-150 (BioLogic.inc, Tokyo, Japan) in a conventional three-electrode cell consisting with a glassy carbon disk electrode (4 mm in diameter), platinum wire and saturated Ag/AgCl as the working, counter and reference electrodes, respectively (EC frontier, Tokyo, Japan).

2.7. Electrochemical detection of SMEnzyme

SMEnzyme from *Bacillus cereus* was mixed with PBS (pH 6.8) with to make final assay concentration from a 10 U mL^{-1} as stock. From this stock solution, calculated amount of SMEnzyme was added to the 2 mL of MB-liposome solution to make the whole concentration from 0.01 – 10 mU mL^{-1} and incubated for 2 min and then DPV was carried out on a potentiostat/galvanostat workstation. To obtain the repeatability, the volume of the MB-liposome in the electrochemical cell always maintain at 2 mL. For the detection in other matrices, the SMEnzyme were initially added in the human plasma, human serum and cell supernatant, collected from the BM5 cell lines, respectively to make the stock concentration. Then the solution was spiked from 0.01 – 10 mU mL^{-1} concentration as previous in the electrochemical cell for the detection measurement.

3. Results and discussion

3.1. Au-PAni/N,S-GQDs nanocomposites and its characterizations

The surface morphology, particle size distribution and fluorescence property of as-prepared N,S-GQDs were first characterized by HRTEM images, given in supplementary information of Fig. S1. The TEM image of as-prepared N,S-GQDs shows the homogenous

distribution and the particle sizes are in the range of 2 – 10 nm with an average diameter of 4.6 ± 0.5 nm, indicating the formation of narrow size-distributed N,S-GQDs, suitable for sensing applications. The fluorescence peak of the as synthesized N,S-GQDs at 450 nm also verified the successful preparation [30, 32]. We have designed the basic electrode material of Au-PAni nanocomposites via interfacial self-oxidation-reduction polymerization method where the aniline monomer in organic layers was only exposed to the $HAuCl_4$ oxidant in aqueous layer and undergo controlled polymerization. This prevents the branching of polyaniline nanowires and arrests the polymer in nanotube form. At the same time, the Au^{3+} ions in aqueous phase were also reduced to its Au^0 state and deposited onto the polyaniline nanowires with homogeneous distribution. In the further step of self-assembly of Au-PAni with N,S-GQDs, the embedded AuNPs have captured the N,S-GQDs via the Au-S bond within the nanocomposites. In the TEM image of the Au-PAni/N,S-GQD in Fig. 1a, the polyaniline nanowires with 30 – 40 nm diameters are observed. The black dots of AuNP which are evenly dispersed within the polymer are also clearly visible in the high magnified image in Fig. 1b. The most interesting part has been revealed in the high resolution TEM image of Au-PAni/N,S-GQD nanocomposites in Fig. 1c which clearly shows two distinct fringes patterns of these two crystalized structures of N,S-GQDs and AuNP, confirming the successful preparation of Au-PAni/N,S-GQD nanocomposites. The AuNPs are ranging over 6 – 14 nm with an average size of 11 ± 0.5 nm inside Au-PAni/N,S-GQD nanocomposites (Fig. 1d) however the GQDs are not observed obviously due to its low dimension and molecular weight.

UV–visible spectra of the nanocomposites are shown in Fig. 1e where the polyaniline chain shows its characteristic peaks at around 320 – 340 nm with a small hump at 410 nm, corresponding to π–π^* transition and excitation transition of benzenoid moiety and polaron transition respectively [33]. The surface plasmon peak of AuNP is intimately combined with polyaniline and clearly represented at 520 nm which further confirmed the very close

aggregation of Au nanoparticles with polyaniline matrix [34]. To confirm the structural property of the Au-PAni/N,S-GQD nanocomposites, XRD analysis was further carried out. The presence of the characteristic peaks of AuNP are clearly visible at 2θ = 38.2°, 44.3°, 64.4° and 77.6° (Fig. 1f), corresponding to the (111), (200), (220) and (311) planes, respectively [35]. Due to the presence of polyaniline nanowires and the graphitic moiety of GQDs, a broad peak has also been observed at 2θ = 24°, revealing the amorphous nature of carbon [36]. It is noteworthy that the addition of carbon-enriched N,S-GQDs does not affect the crystal pattern of the AuNP even after the gold thiol bonding which can maintain the electroactive nature of the nanocomposites while using for the electrochemical studies.

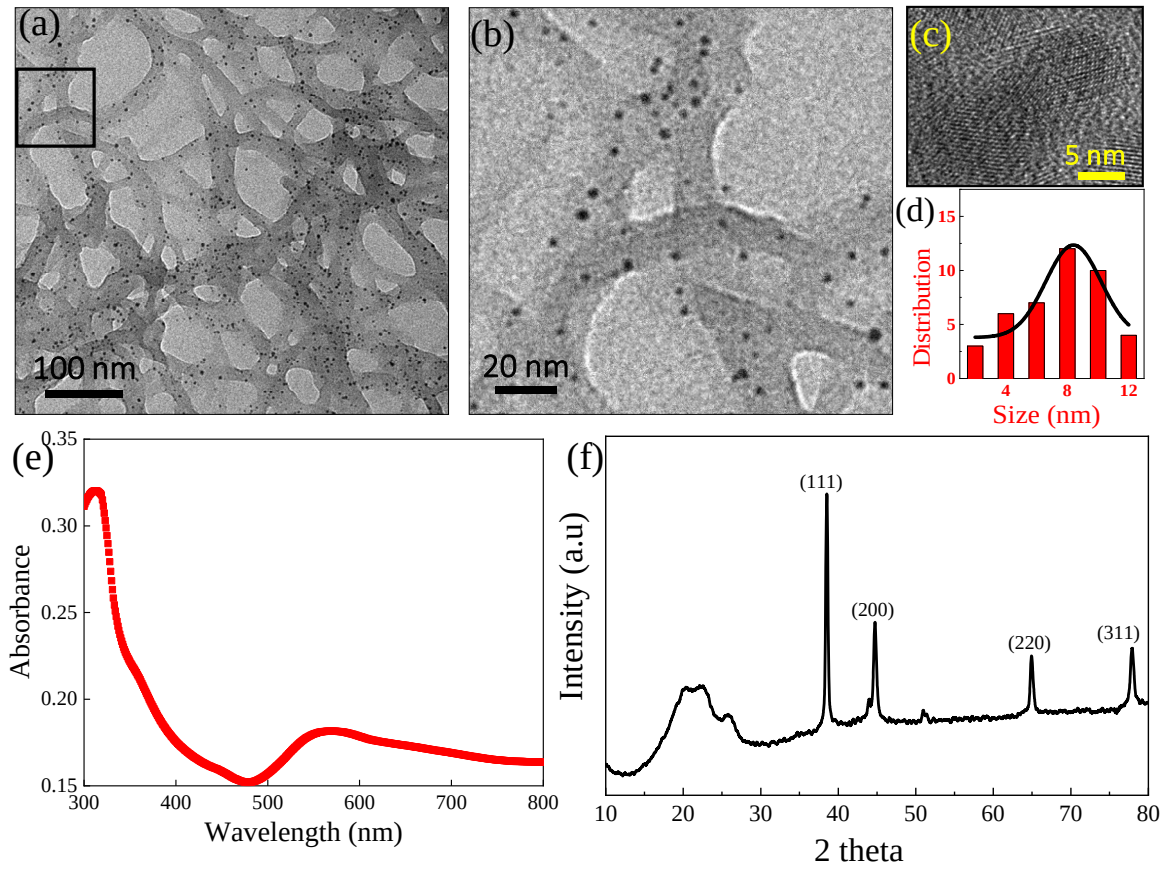

Fig. 1. Characterizations of Au-PAni/N,S-GQD nanocomposites: (a) TEM image, (b) high magnified TEM image of AuNP on the PAni chain, (c) high resolution TEM image of the Au-

PAni/N,S-GQD nanocomposites, showing the fringes of GQDs and AuNP, (d) size distribution of the AuNP inside of the AuNP-PAni nanocomposites, (e) UV-Vis spectrum of Au-PAni/N,S-GQD nanocomposites, and (F) XRD of Au-PAni/N,S-GQD nanocomposites.

3.2. MB-liposome formulation and its optimized condition for SMEnzyme detection

The most challenging task in any liposome-based assays is the liposomal formulation which should be intrinsically nonpermeable and stable over a long period of time. In addition, the liposome should contain maximum amount of analyzing molecules inside its cavity as well as highly sensitive towards the target molecules. To investigate these several optimizing conditions, we have used the 0.1 – 10 mU mL^{-1} SMEnzyme as a standard target concentration throughout the whole optimizing process [9]. Initially, we focused on producing non-leaky liposomes, varying the molecular ratio of SM and cholesterol within the liquid ordered state. The MB containing liposomes were prepared using conventional lipid film hydration. Then free MB molecules were removed from the liposome suspension by repeated ultracentrifugation at 10000 × g. Three different molar ratios of SM:Cholesterol are chosen as 30:70, 50:50 and 70:30 and treated them with 0.1 – 10 mU mL^{-1} of SMEnzyme. In case of 50:50 and 70:30, the calibration lines are found extremely well compared to the 30:70 compositions. However, the 70:30 molar ratio mixtures had a slightly higher background leakage. In case of 30:70, the calibration line is highly scattered which may be due to the high amount of cholesterol which can loosen the structure of SM-based liposome, resulting leakage. Though the high amount of SM compared with cholesterol shows similar results with its 50:50 ratios, however, the initial peak intensity of the MB is smaller in case of 50:50 ratio (Fig. 2a), indicating minimum leakage or background signal when no enzyme was added. Therefore, SM:Cholesterol of 50:50 appeared to be the optimal lipid composition for further study.

Next, the loading of MB concentration was investigated with the optimized 50:50 SM:Cholesterol liposome. During the liposomal synthesis, 4 concentrations of MB (0.1, 1, 5 and 10 mM) has been used to encapsulate inside liposome and then tested with 0.1 – 10 mU mL^{-1} SMEnzyme. It is evident from Fig. 2b that except 0.1 mM, all concentrations of MB show significant peak intensity in DPV signal with linear calibration. As the concentration of the treated enzyme is quite high in this condition, sufficiently high peak current is highly desirable for low level detection of SMEnzyme in further cases. Therefore, the smallest amount of 0.1 mM MB should be rejected. Compared with all three high concentrated MB-encapsulated liposomes, the overall peak intensities of the calibration line of 1 mM MB is quite comparable with the other two concentration (5 and 10 mM). As the high concentration of MB-loaded liposomes are difficult to purify and the 1 mM MB liposome also provide sufficient signal in DPV, we have chosen this concentration as optimum for all further studies. Similarly, the incubation time of the SMEnzyme with 1 mM MB-loaded liposome of 50:50 ratio (SM:Cholesterol) are further investigated to obtain the optimum time of reaction. As shown in Fig. 2c, after incubation with the 1 mM SMEnzyme as a standard concentration of target with the MB-liposome, the peak current of the DPV increases rapidly up to 120 sec and then tends to the saturation, indicating the end point of the reaction. It suggests the optimum incubation time for the further studies for SMEnzyme detection should be 120 sec. The reaction between the sphingomyelin and sphingomyelinase is an enzymatic process which is quite fast as obvious as any other enzymatic reaction. Therefore, after adding the enzyme on the SM-liposome solution, it converts the SM to ceramide rapidly and make the rupture of the liposomal formation, releasing all the encapsulated MB into solution. Then the released MB has been adsorbed on the GQD attached electrode surface where the whole process takes an approximate time of 120 sec. After separation of MB-liposome from excess MB by centrifugation, the MB-liposomes are analyzed by different characterization tools like DLS, TEM etc. to study its

structural or physical properties. As the structural property is highly important and influential to the chemical properties of the liposome, the effect of liposomal size on the SMEnzyme assay has been also investigated. We have used a 100 nm pore sized polycarbonate membrane to separate the as synthesized MB-liposome to get uniform distribution. When the as prepared and the size normalized MB-liposomes are treated with 0.1 – 10 mU mL^{-1} of SMEnzyme, the sensitivity in the DPV peak has changed significantly. We observed that the 100 nm or less sized liposomes showed a limit of detection, calculated by 3σ/s method (three times of the standard deviation of the lowest concentration of target/slope of the calibration line) of 7.2 μU mL^{-1} compared with 14.8 μU mL^{-1} in the case of as synthesized liposomes (Fig. 2d). There are few reports on the advancement procedures of SMEnzyme detection which are listed in the Table 1. In recent study, most of the reports are mainly demonstrated on the SMEnzyme activity measurement by different methodologies like radiolabeled, fluorometric, colorimetric assays etc., but the quantification is rarely reported. Summarizing in Table 1, the sensitivity in term of detection range and limit of detection, the current work shows superior performance compared to other methods.

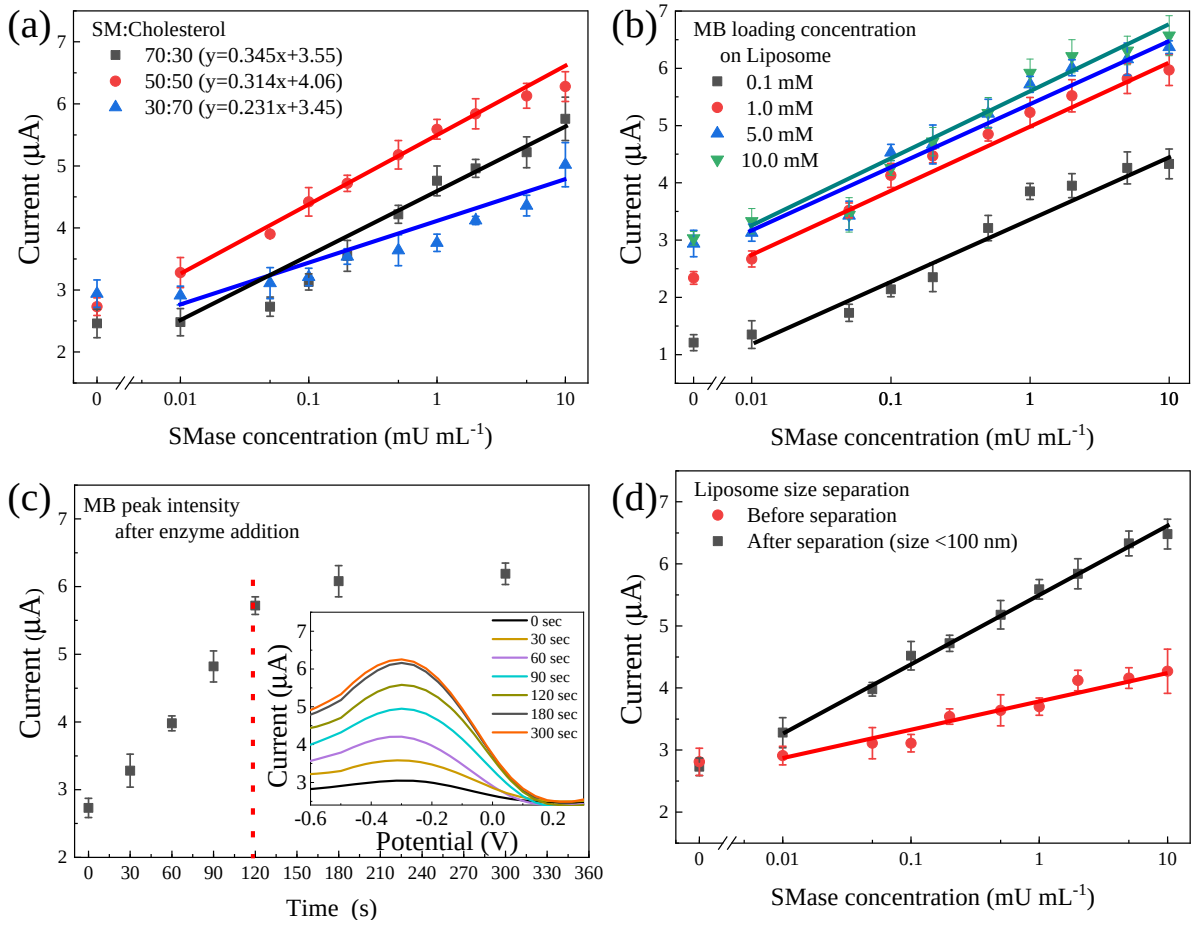

Fig. 2. Effect of lipid-cholesterol composition, MB concentration loading, time of incubation of SMEnzyme and diameter on SMEnzyme detection: (a) effect of SM:Cholesterol ratios of 30:70, 50:50 and 70:30, (b) effect of MB loading concentration of 0.1, 1, 5, 10 mM, (c) time of incubation for DPV analysis and (d) effect of 100 nm size separation of MB-liposome.

Table 1

Comparison of the sensitivity of the current method with previously reported other mythologies of SMEnzyme detection.

Methods	Detection range	Detection limit	Reference
Liposome based colorimetric	0.01 – 10 mU mL^{-1}	0.02 mU mL^{-1}	[9]

Well plate assay	10 – 120 nM	10 nM	[10]
C^{14} Radiolabeled	5 – 2.5 mU mL^{-1}	5 mU mL^{-1}	[37]
Fluorescence based HPLC	2.5 – 97.4 pmol mL^{-1} h^{-1}	36.0 pmol mL^{-1} h^{-1}	[38]
Liposome based electrochemical	0.1 – 10 mU mL^{-1}	0.0072 mU mL^{-1}	This work

The purified size distribution was also analyzed by TEM images (Fig. 3a-c) and DLS measurements (Fig. 3d). The TEM image of as synthesized MB-liposome in Fig. 3a showed scattered liposomal distribution in a very wide range of sizes (70 – 300 nm) whereas the distribution became predominantly uniformed after the size purification in Fig. 3b. In addition, the spherical vesicles are also clearly observed with mean diameter of 101.5 ± 2.5 nm, shown in the inset of Fig. 3b. When the MB-liposome was treated with the 1 mU mL^{-1} of SMEnzyme and the sample was taken after 10 min, the grid became almost vacant (Fig. 3c), indicating the successful rupture of all MB-liposome. These observations confirm the disruption of liposomes upon addition of SMEnzyme on this SM:cholesterol 50:50 liposome formulation. To re-confirm the phenomenon, hydrodynamic radii of different stages of MB-liposome are also determined using dynamic light scattering (DLS), given in Fig. 3d. The average size of the as synthesized MB-liposome was found of 112.2 nm (PDI 0.27) which was reduced to 92.5 nm (PDI 0.21) for size neutralized liposome. However, after treatment with the SMEnzyme, the particle counts were dramatically decreased, indicating the rupture of the liposome which completely corroborated with the finding in TEM. The MB peak responses in DPV of these three conditioned MB-liposome are also given in Fig. 3e where the MB peak only can be observed significantly after the treatment of SMEnzyme which supports our hypothesis. Additionally, the stability of the MB-liposome was also analyzed in DPV without any enzyme over 1 h in the reaction buffer of PBS containing 1 mM $MgSO_4$, and $CaCl_2$ (Fig. S2) which

proves the MB-liposome can be a good matrix for this sensing purpose. Summarizing the above optimizations, we can conclude that the MB-liposome with SM:cholesterol ratio of 50:50 with 100 nm diameter with 1 mM-encapsulated MB should be the most suitable composition for the SMEnzyme assays with a response time of 120 sec.

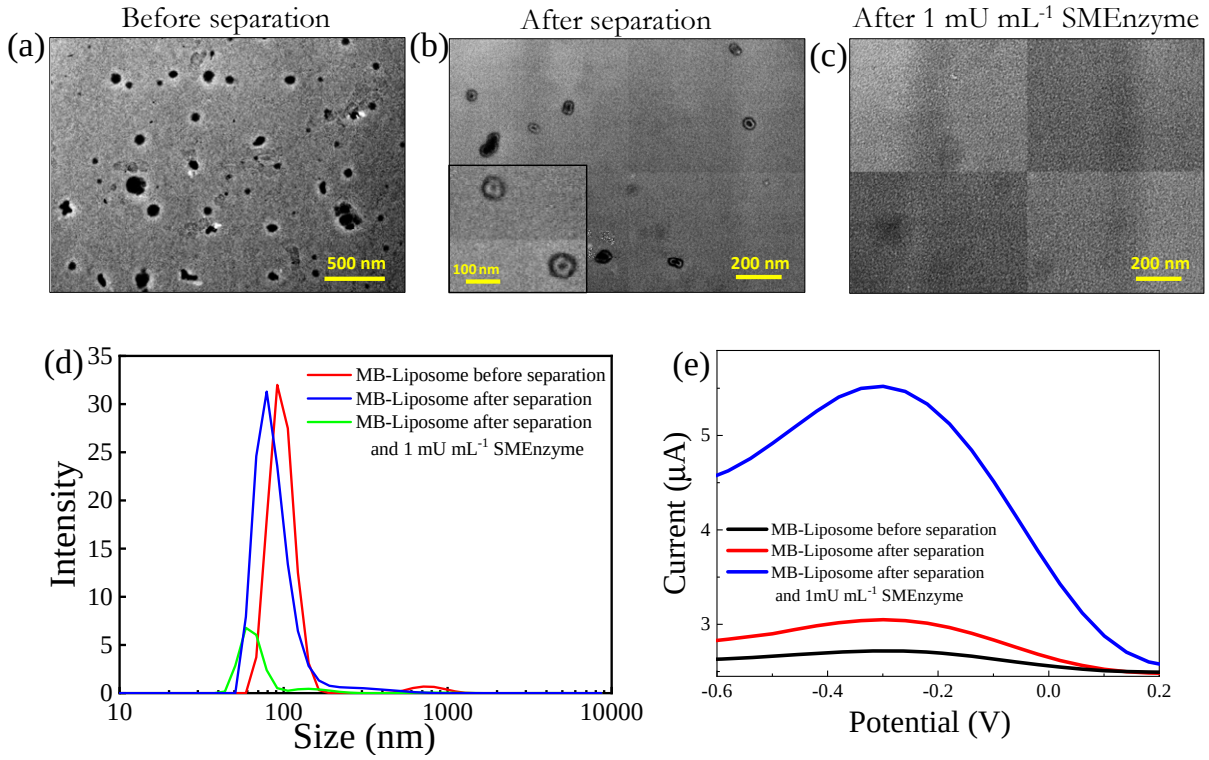

Fig. 3. (a) TEM images of MB-liposomes before separation, (b) after separation with 100 nm membrane and (c) after treated with 1 mU mL^{-1} SMEnzyme on 100 nm separated MB-liposome, (d) DLS measurement to identify the particle sizes of MB-liposomes before and after separation, and after treated with 1 mU mL^{-1} SMEnzyme, (e) DPV peak intensity found from the released MB of MB-liposomes before and after separation, and after treated with 1 mU mL^{-1} SMEnzyme.

3.3. Electrochemical detection of SMEnzyme

After accumulating all optimizing conditions for SMEnzyme detection, the MB-liposome has been applied to detect different concentration of SMEnzyme and make the calibration lines, shown in Fig. 4. The bare MB-liposome was treated in the electrochemical cell where the working GCE was drop-casted with Au-PAni/N,S-GQD nanocomposite. According to the hypothesis, after addition of the triggering target SMEnzyme into the liposomal solution, it oxidized the SM to ceramide and perturbed the liposomal structure, making release of encapsulated MB into the buffer solution. The graphitic structure of N,S-GQD in the working electrode easily adsorbed the released MB and hence shows the peak in DPV. As a small amount of the SMEnzyme can spill a comparatively large sized liposome, containing MB as a redox indicator, the released MB easily amplify the signal in DPV which is the key point of this study. As shown in Fig. 4a, the DPV signal of MB at -0.3 V clearly represented the presence of SMEnzyme in the concentration range of 0.01 – 10 mU mL^{-1}. The calibration line established from the peak current in DPV has been plotted in Fig. 3b which maintains the linearity over the wide concentration range with the correlation coefficient of 0.982. The detection limit was found from the calibration line of 7.2 μU mL^{-1}, calculated from 3σ/s method (three times of the standard deviation of the lowest concentration of target/slope of the calibration line) [39]. Due to the liposomal amplification and high sensitive electrochemical process, this assay achieves much better sensitivity than the commercially available assay kits [10, 38], in a small response time of only 2 min.

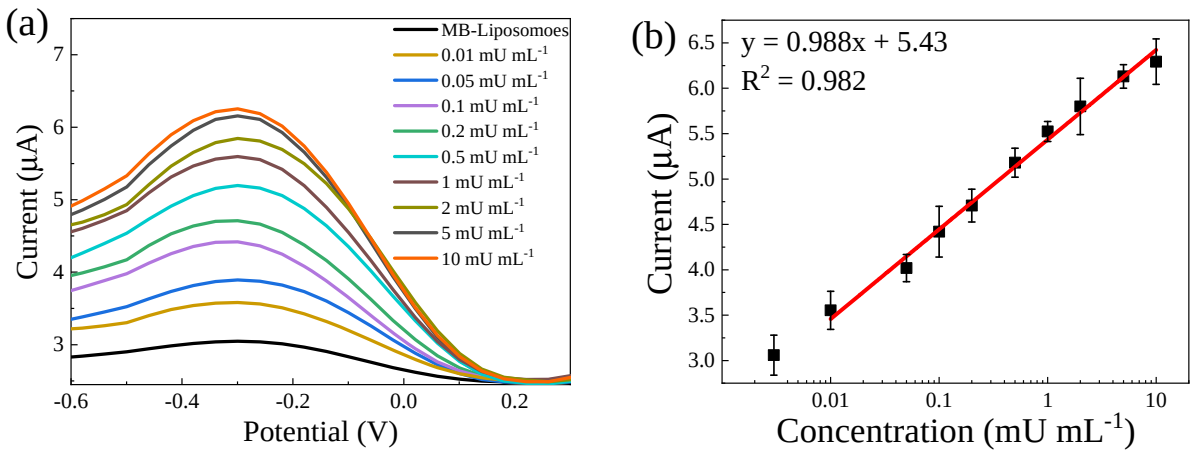

Fig. 4. Detection of SMEnzyme in DPV: (a) redox peak of MB, released from the MB-liposome after treated with the SMEnzyme in the concentration range of 0.01 – 10 mU mL^{-1}, (b) calibration line of MB peak intensities vs concentration of SMEnzyme.

3.4. Specificity and selectivity of the liposome-based assay

To confirm our sensing specificity of SMEnzyme with the MB-liposome, we performed control experiments in different conditions with and without SMEnzyme and other proteins. As the SM oxidation by SMEnzyme is already well-established fact in term of specificity, it is expected to get high specific nature of this sensing study. However, to verify the SM-liposome stability in different condition, we have carried out the following selectivity test. Blank liposome (without any MB loading, only buffer loaded) and MB-liposomes had incubated with the SMEnzyme of 1 mU mL^{-1} and surfactant Triton X100 as positive control (Fig. 5a). The liposomes (as negative control) did not show any signal in DPV, confirming the stable structure. After addition of 1 mU mL^{-1} SMEnzyme, there was an obvious peak generated from MB-liposome while the bare liposome showed nothing. It can prove that the MB signal is only come from the MB-encapsulated liposomal matrix. In case of positive control of Triton X, similar observation was noted, confirming the reaction mechanism. When the MB-liposome was

treated with other possible interferences of bovine serum albumin (BSA), lysozyme (Lys) and phospholipase A, the DPV signal did not show any significant peak, indicating the inert activity with the MB-liposome (Fig. 5b). As expected, there was no change in peak current of the control on incubation of MB-liposomes with lysozyme and BSA, confirming that MB release is not induced by any protein adsorption onto the liposome surface. Therefore, the release of MB is specifically driven by the oxidation of MB-liposome of SM by the activity of SMEnzyme.

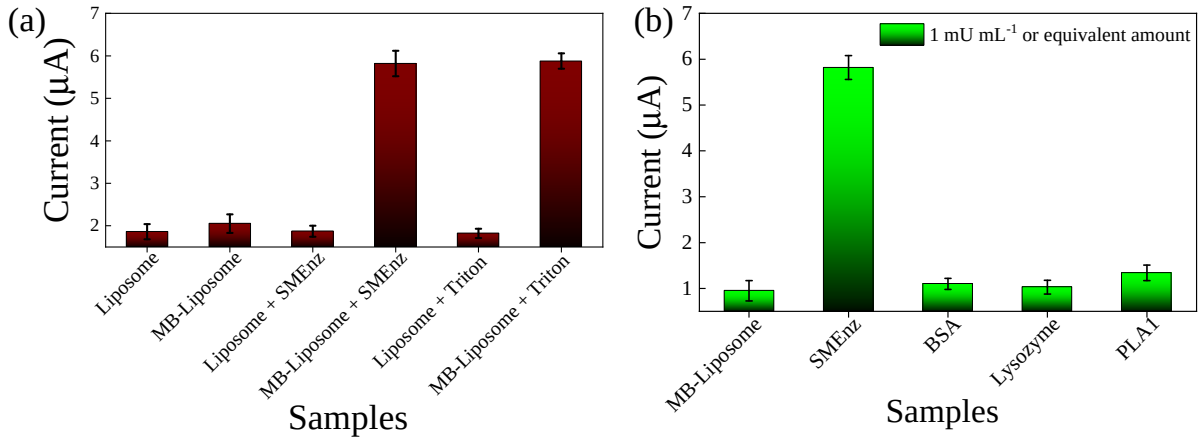

Fig. 5. Specificity and selectivity of SMEnzyme detection of 1mM MB encapsulated MB-liposome. (a) DPV peak signal at -0.3V for bare liposome and MB-liposome while treated with SMEnzyme and Triton X (b) specificity of the assay toward SMEnzyme, lysozyme, BSA, and phospholipase A. Incubation times were 2 min for all measurements.

3.5. Effect of matrices on the sensor performance for the real time monitoring

To confirm the practicability of this proposed method, analyzing detection ability in other possible matrices is extremely important. Therefore, performances of the biosensor were investigated in the spiked concentration of SMEnzyme in human serum, human plasma and cell culture supernatant and then compared with the calibration line in PBS medium, as shown

in Fig. 6. The presence of large amount of unspecified proteins in the serum and plasma matrices leads to some nonspecific interaction with the sensor, resulting in a relatively large blank value compared to PBS (Fig. 6). However, in case of cell supernatant, the effect is almost ignorable. In addition, although the calibration lines show the same trends as before, their slopes have been decreased in some extend, resulting the decreasing of sensitivity. The LODs have been calculated from their calibration lines which are 14.5 µU mL^{-1} in cell supernatant, 19.5 µU mL^{-1} in human serum and 32.4 µU mL^{-1} in human plasma. The sensitivity has some obvious decreased due to the presence of large interferences in these matrices compared to the PBS system however it is quite satisfactory for the application in real time monitoring.

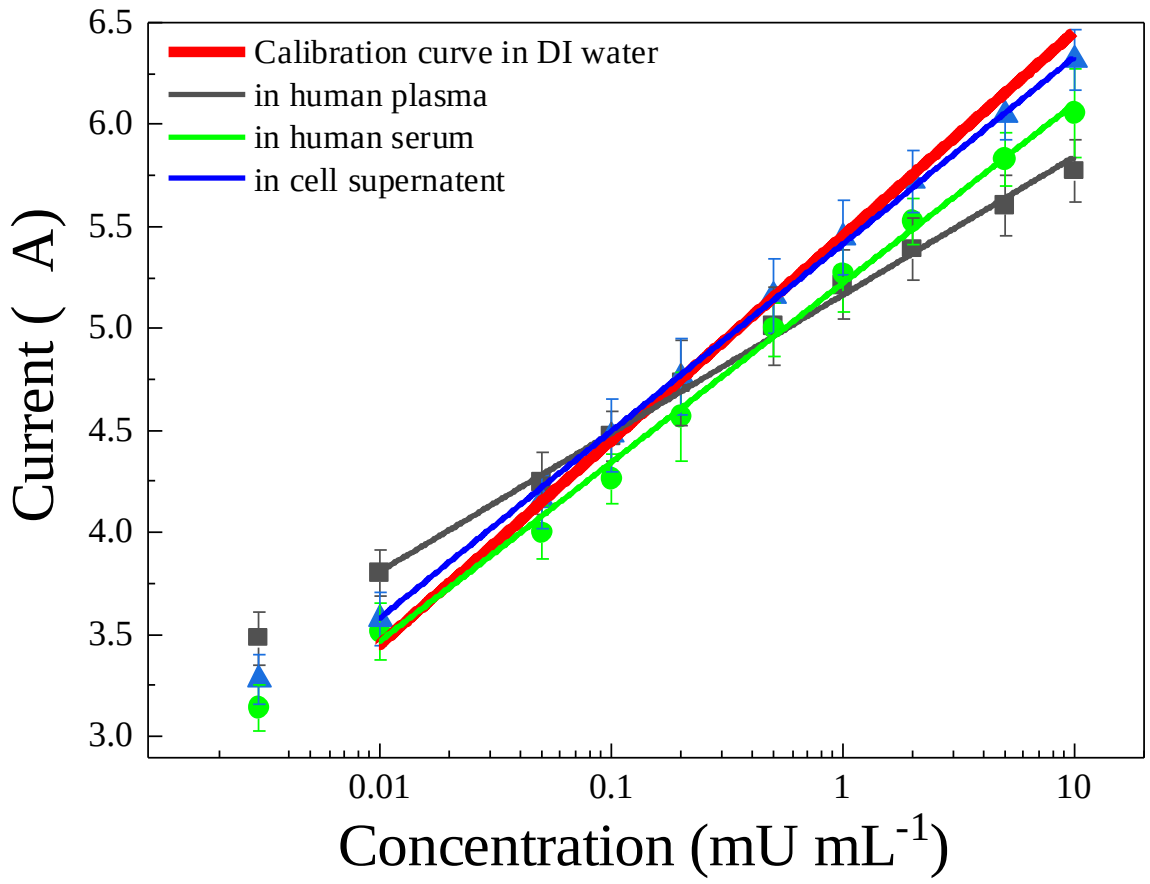

Fig. 6. Peak current of MB for the detection of SMEnzyme: Calibration lines in human plasma (closed squares), human serum (closed circles) and cell supernatant (closed triangles) vs concentration of SMEnzyme. The calibration line in PBS is also plotted for comparison.

4. Conclusion

The central theme of this work has been schematically presented in scheme where the new class of liposomes was formulated with 50:50 SM and cholesterol, encapsulated with 1mM MB as redox indicator for the electrochemical DPV detection of SMEnzyme. Using liposomes formulated from SM to detect SMEnzyme offers a cell-membrane mimicking environment for the enzymatic activity. Using this assay, the SMEnzyme causes the perturbation of MB-liposome, resulting free release of the MB which successfully detected by GCE||Au-PAni/N,S-GQDs working electrode in electrochemical cell in DPV process with the detection limit of 7.2 μU mL^{-1} that is quite lower than the commercially available SMEnzymatic assays. In addition, minimal cross-reactivity with similar phospholipase and other possible interfering proteins confirmed the stable and non-leaky structure of MB-liposome with low background noise and high specific nature. Finally, the applicability of the proposed sensor has successfully verified in three possible sources of the SMEnzyme where the obtained LOD has been found 14.5 μU mL^{-1} in cell supernatant, 19.5 μU mL^{-1} in human serum and 32.4 μU mL^{-1} in human plasma which is quite satisfactory for its real application. We can expect from the above finding that this sensing system can have that potential for the usage in both point-of-care diagnosis and high throughput pharmaceutical screening in future.

Declaration of competing interest

The authors declare no competing financial interest.

Acknowledgement

A.D.C. sincerely thanks the Japan Society for the Promotion of Science (JSPS) for a postdoctoral fellowship (Grant Nos. P17359).

Appendix A. Supplementary data

Supplementary material related to this article can be found, in the online version, at doi:https://doi.org/.

References

[1] J.P. Slotte, B. Ramstedt, The functional role of sphingomyelin in cell membranes, Eur J Lipid Sci Technol, 109(2007) 977-81.

[2] T. Kolter, K. Sandhoff, Sphingolipids—their metabolic pathways and the pathobiochemistry of neurodegenerative diseases, Angew Chem Int Ed, 38(1999) 1532-68.

[3] J. Kornhuber, C. Rhein, C.P. Müller, C. Mühle, Secretory sphingomyelinase in health and disease, Biol Chem, 396(2015) 707-36.

[4] A.H. Futerman, Y.A. Hannun, The complex life of simple sphingolipids, EMBO Rep, 5(2004) 777-82.

[5] E.H. Schuchman, M.P. Wasserstein, Types A and B Niemann-Pick disease, Best Pract Res Clin Endocrinol Metab, 29(2015) 237-47.

[6] E. Gulbins, M. Palmada, M. Reichel, A. Lüth, C. Böhmer, D. Amato, et al., Acid sphingomyelinase–ceramide system mediates effects of antidepressant drugs, Nat Med, 19(2013) 934.

[7] M. Figuera-Losada, M. Stathis, J.M. Dorskind, A.G. Thomas, V.V.R. Bandaru, S.W. Yoo, et al., Cambinol, a novel inhibitor of neutral sphingomyelinase 2 shows neuroprotective properties, PLoS One, 10(2015) e0124481.

[8] T. Pinkert, D. Furkert, T. Korte, A. Herrmann, C. Arenz, Amplification of a FRET Probe by Lipid–Water Partition for the Detection of Acid Sphingomyelinase in Live Cells, Angew Chem Int Ed, 56(2017) 2790-4.

[9] M.N. Holme, S. Rana, H.M. Barriga, U. Kauscher, N.J. Brooks, M.M. Stevens, A robust liposomal platform for direct colorimetric detection of sphingomyelinase enzyme and inhibitors, ACS Nano, 12(2018) 8197-207.

[10] M. Xu, K. Liu, N. Southall, J.J. Marugan, A.T. Remaley, W. Zheng, A high-throughput sphingomyelinase assay using natural substrate, Analytical and bioanalytical chemistry, 404(2012) 407-14.

[11] F. Ghomashchi, M. Barcenas, F. Turecek, C.R. Scott, M.H. Gelb, Reliable assay of acid sphingomyelinase deficiency with the mutation Q292K by tandem mass spectrometry, Clin Chem, 61(2015) 771-2.

[12] B. Liu, Y.A. Hannun, Sphingomyelinase assay using radiolabeled substrate, Methods Enzymol, Elsevier 2000, 164-7.

[13] L. Di Marzio, A. Di Leo, B. Cinque, D. Fanini, A. Agnifili, P. Berloco, et al., Detection of alkaline sphingomyelinase activity in human stool: proposed role as a new diagnostic and prognostic marker of colorectal cancer, Cancer Epidemiol Biomarkers Prev, 14 (2005) 856-62.

[14] M.B. Ruiz-Argüello, M.P. Veiga, J.L. Arrondo, F.M. Goñi, A. Alonso, Sphingomyelinase cleavage of sphingomyelin in pure and mixed lipid membranes. Influence of the physical state of the sphingolipid, Chem Phys Lipids, 114(2002) 11-20.

[15] F.-X. Contreras, J. Sot, M.-B. Ruiz-Argüello, A. Alonso, F. Goni, Cholesterol modulation of sphingomyelinase activity at physiological temperatures, Chem Phys Lipids, 130(2004) 127-34.

[16] D. Aili, M. Mager, D. Roche, M.M. Stevens, Hybrid nanoparticle− liposome detection of phospholipase activity, Nano Lett, 11(2010) 1401-5.

[17] N.J. Liu, R. Chapman, Y. Lin, J. Mmesi, A. Bentham, M. Tyreman, et al., Point of care testing of phospholipase A2 group IIA for serological diagnosis of rheumatoid arthritis, Nanoscale, 8(2016) 4482-5.

[18] A.D. Chowdhury, A.B. Ganganboina, Y.-c. Tsai, H.-c. Chiu, R.-a. Doong, Multifunctional GQDs-Concanavalin A@ Fe_3O_4 nanocomposites for cancer cells detection and targeted drug delivery, Anal Chim Acta, 1027(2018) 109-20.

[19] S. Dutta, A.D. Chowdhury, S. Biswas, E.Y. Park, N. Agnihotri, A. De, et al., Development of an effective electrochemical platform for highly sensitive DNA detection using MoS_2-polyaniline nanocomposites, Biochem Eng J, 140(2018) 130-9.

[20] A.D. Chowdhury, A.B. Ganganboina, E.Y. Park, R.A. Doong, Impedimetric biosensor for detection of cancer cells employing carbohydrate targeting ability of Concanavalin A, Biosensors Bioelectron, 122(2018) 95-103.

[21] A. Dutta Chowdhury, A.B. Ganganboina, F. Nasrin, K. Takemura, R.A. Doong, D.I.S. Utomo, et al., Femtomolar detection of dengue virus DNA with serotype identification ability, Anal Chem, 90(2018) 12464-74.

[22] A.D. Chowdhury, R. Gangopadhyay, A. De, Highly sensitive electrochemical biosensor for glucose, DNA and protein using gold-polyaniline nanocomposites as a common matrix, Sensors Actuators B: Chem, 190(2014) 348-56.

[23] E. Paleček, F. Jelen, Electrochemistry of nucleic acids and development of DNA sensors, Crit Rev Anal Chem, 32(2002) 261-70.

[24] U. Bogdanovic, I. Pašti, G. Ciric-Marjanovic, M. Mitric, S.P. Ahrenkiel, V. Vodnik, Interfacial synthesis of gold–polyaniline nanocomposite and its electrocatalytic application, ACS Appl Mater Interfaces, 7(2015) 28393-403.

[25] Q. Hao, H. Wang, X. Yang, L. Lu, X. Wang, Morphology-controlled fabrication of sulfonated graphene/polyaniline nanocomposites by liquid/liquid interfacial polymerization and investigation of their electrochemical properties, Nano Research, 4(2011) 323-33.

[26] D. Zhai, B. Liu, Y. Shi, L. Pan, Y. Wang, W. Li, et al., Highly sensitive glucose sensor based on Pt nanoparticle/polyaniline hydrogel heterostructures, ACS Nano, 7(2013) 3540-6.

[27] C. Xia, X. Hai, X.-W. Chen, J.-H. Wang, Simultaneously fabrication of free and solidified N, S-doped graphene quantum dots via a facile solvent-free synthesis route for fluorescent detection, Talanta, 168(2017) 269-78.

[28] T. Liu, Y. Li, Q. Du, J. Sun, Y. Jiao, G. Yang, et al., Adsorption of methylene blue from aqueous solution by graphene, Colloids Surf B Biointerfaces, 90(2012) 197-203.

[29] K. Mao, D. Wu, Y. Li, H. Ma, Z. Ni, H. Yu, et al., Label-free electrochemical immunosensor based on graphene/methylene blue nanocomposite, Anal Biochem, 422(2012) 22-7.

[30] N.T.N. Anh, A.D. Chowdhury, R.-a. Doong, Highly sensitive and selective detection of mercury ions using N, S-codoped graphene quantum dots and its paper strip based sensing application in wastewater, Sensors Actuators B: Chem, 252(2017) 1169-78.

[31] R. Gangopadhyay, A.D. Chowdhury, A. De, Functionalized polyaniline nanowires for biosensing, Sensors Actuators B: Chem, 171(2012) 777-85.

[32] Y. Dong, H. Pang, H.B. Yang, C. Guo, J. Shao, Y. Chi, et al., Carbon based dots co doped with nitrogen and sulfur for high quantum yield and excitation independent emission, Angew Chem, 125(2013) 7954-8.

[33] J. Han, L. Li, R. Guo, Novel approach to controllable synthesis of gold nanoparticles supported on polyaniline nanofibers, Macromolecules, 43(2010) 10636-44.

[34] K. Kalishwaralal, V. Deepak, S.R.K. Pandian, M. Kottaisamy, S. BarathManiKanth, B. Kartikeyan, et al., Biosynthesis of silver and gold nanoparticles using Brevibacterium casei, Colloids Surf B Biointerfaces, 77(2010) 257-62.

[35] K. Dave, K.H. Park, M. Dhayal, Characteristics of ultrasonication assisted assembly of gold nanoparticles in hydrazine reduced graphene oxide, RSC Adv, 5(2015) 107348-54.

[36] T. Berzina, A. Pucci, G. Ruggeri, V. Erokhin, M.P. Fontana, Gold nanoparticles–polyaniline composite material: Synthesis, structure and electrical properties, Synth Met, 161(2011) 1408-13.

[37] T. Taki, S. Chatterjee, An improved assay method for the measurement and detection of sphingomyelinase activity, Analytical biochemistry, 224(1995) 490-3.

[38] X. He, F. Chen, A. Dagan, S. Gatt, E.H. Schuchman, A fluorescence-based, high-performance liquid chromatographic assay to determine acid sphingomyelinase activity and diagnose types A and B Niemann–Pick disease, Analytical biochemistry, 314(2003) 116-20.

[39] A. Dutta Chowdhury, R.A. Doong, Highly sensitive and selective detection of nanomolar ferric ions using dopamine functionalized graphene quantum dots, ACS Appl Mater Interfaces, 8(2016) 21002-10.

Chowdhury et al., Scheme 1

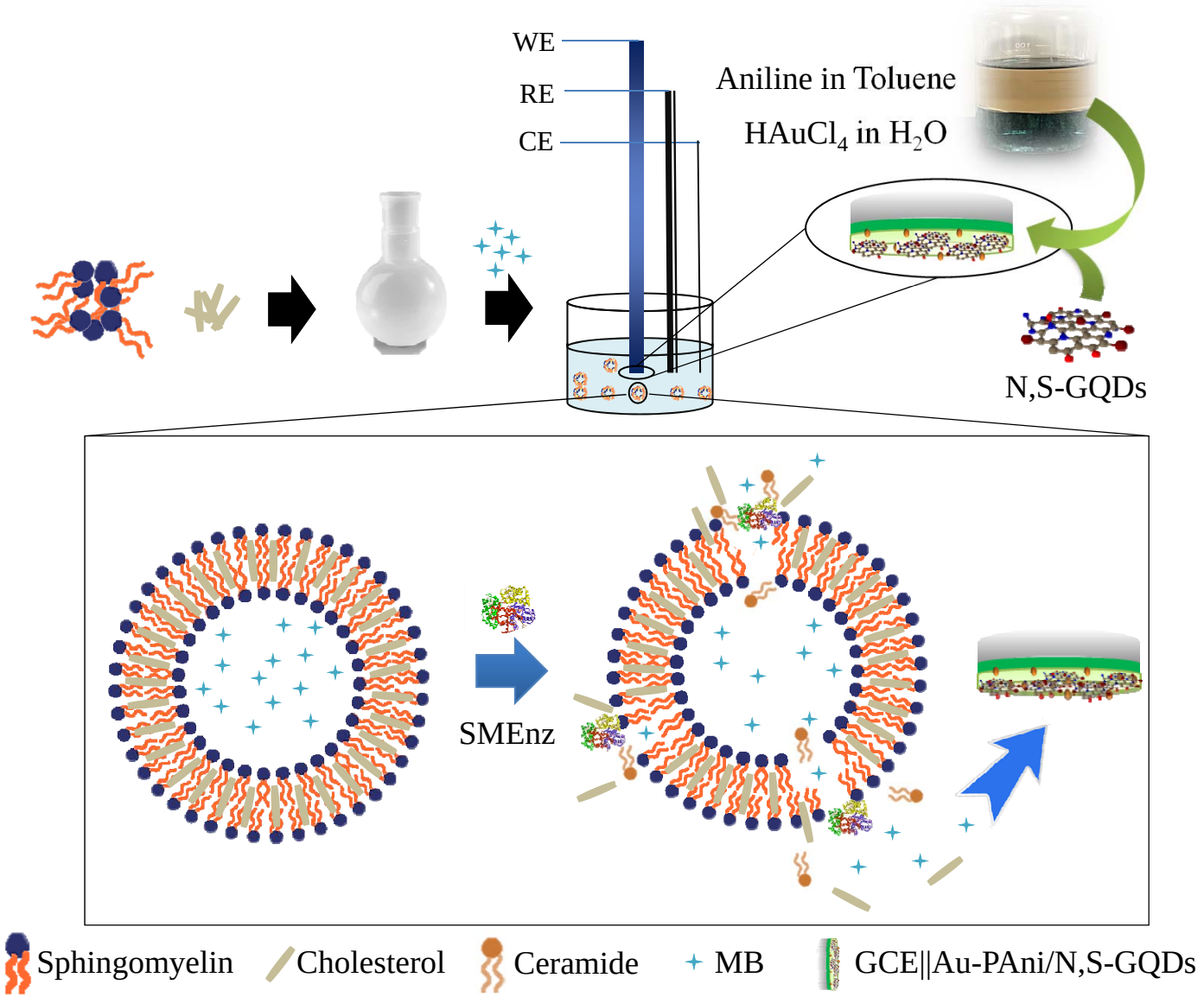

Chowdhury et al., Fig.1

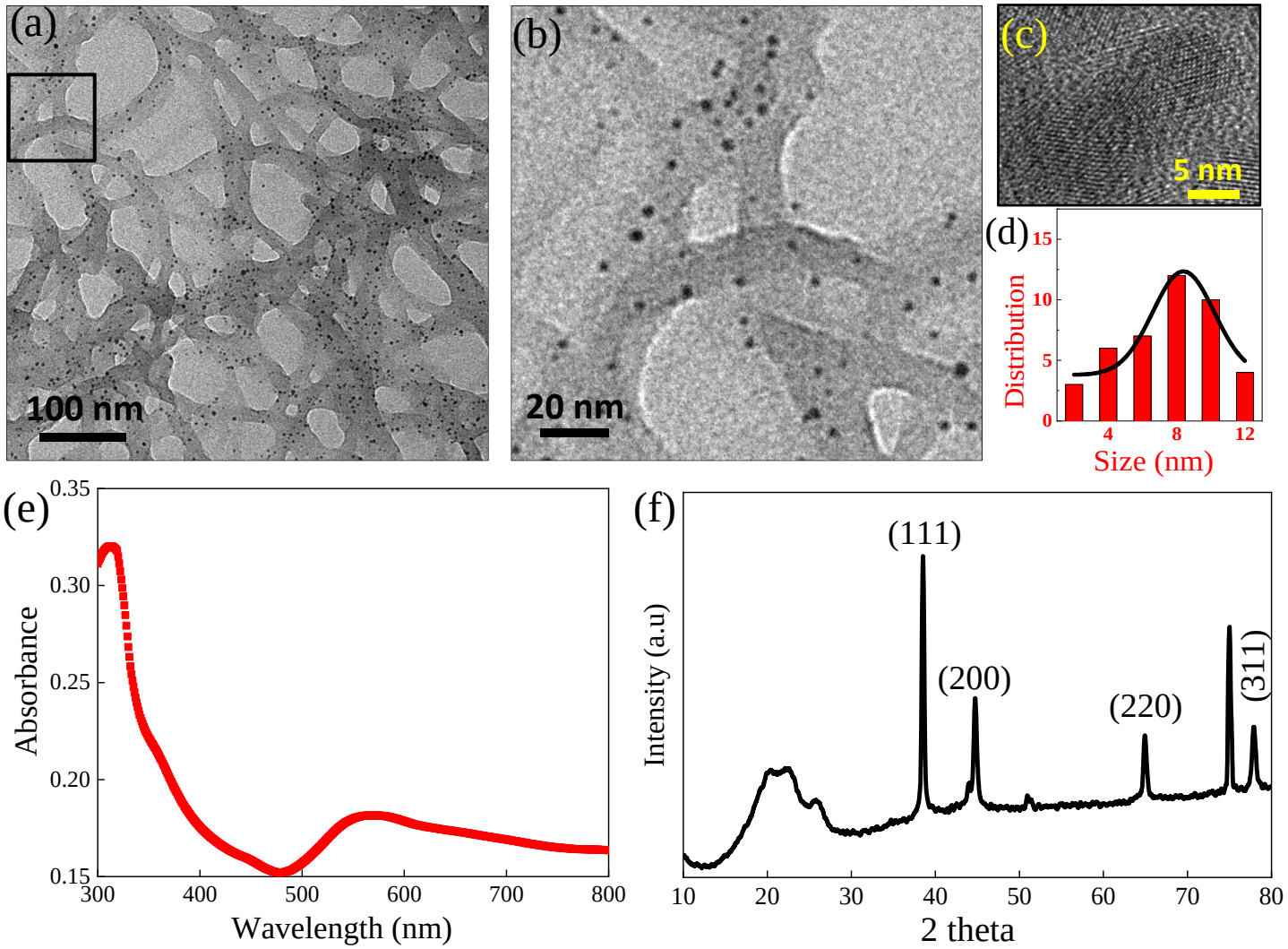

Chowdhury et al., Fig. 2

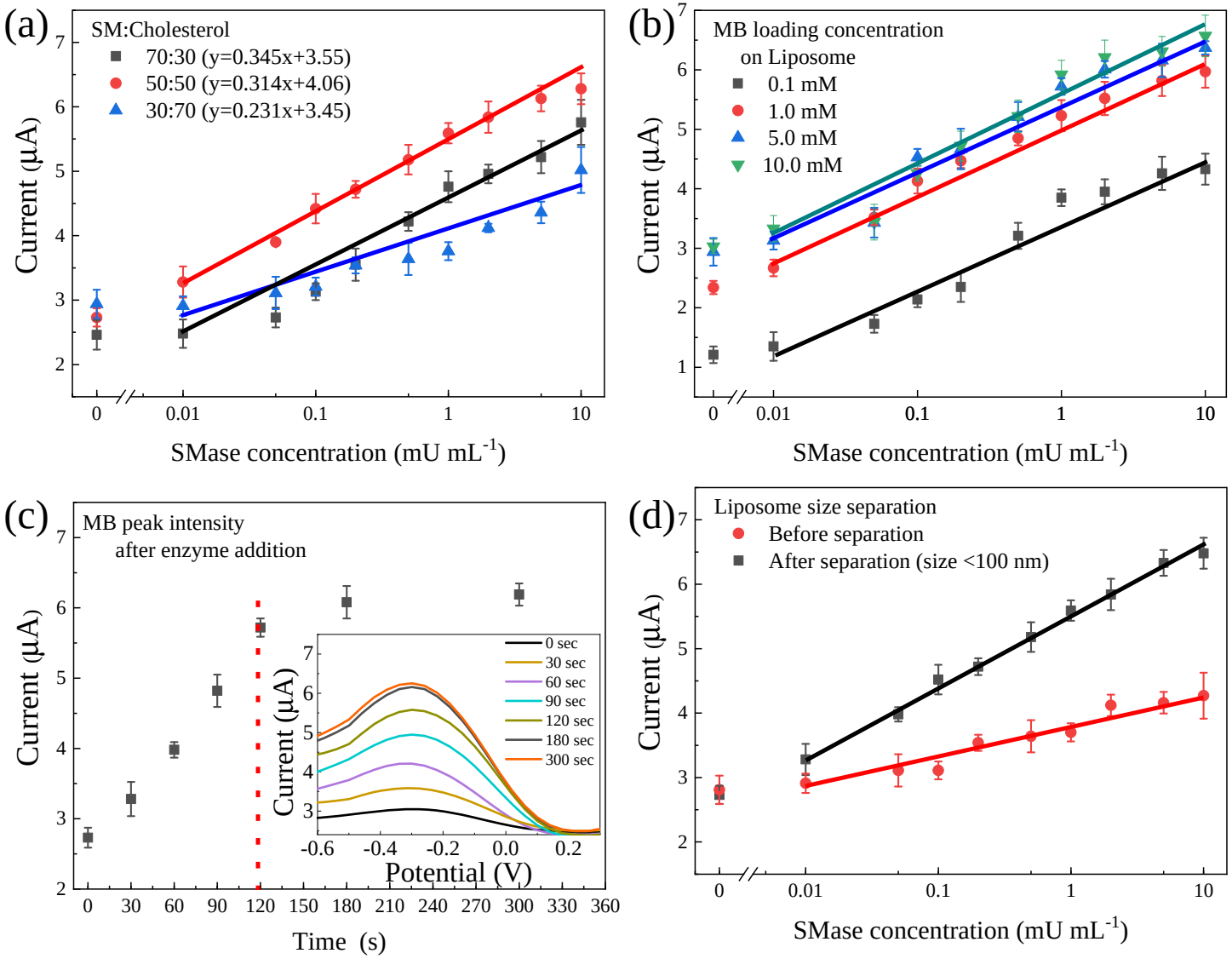

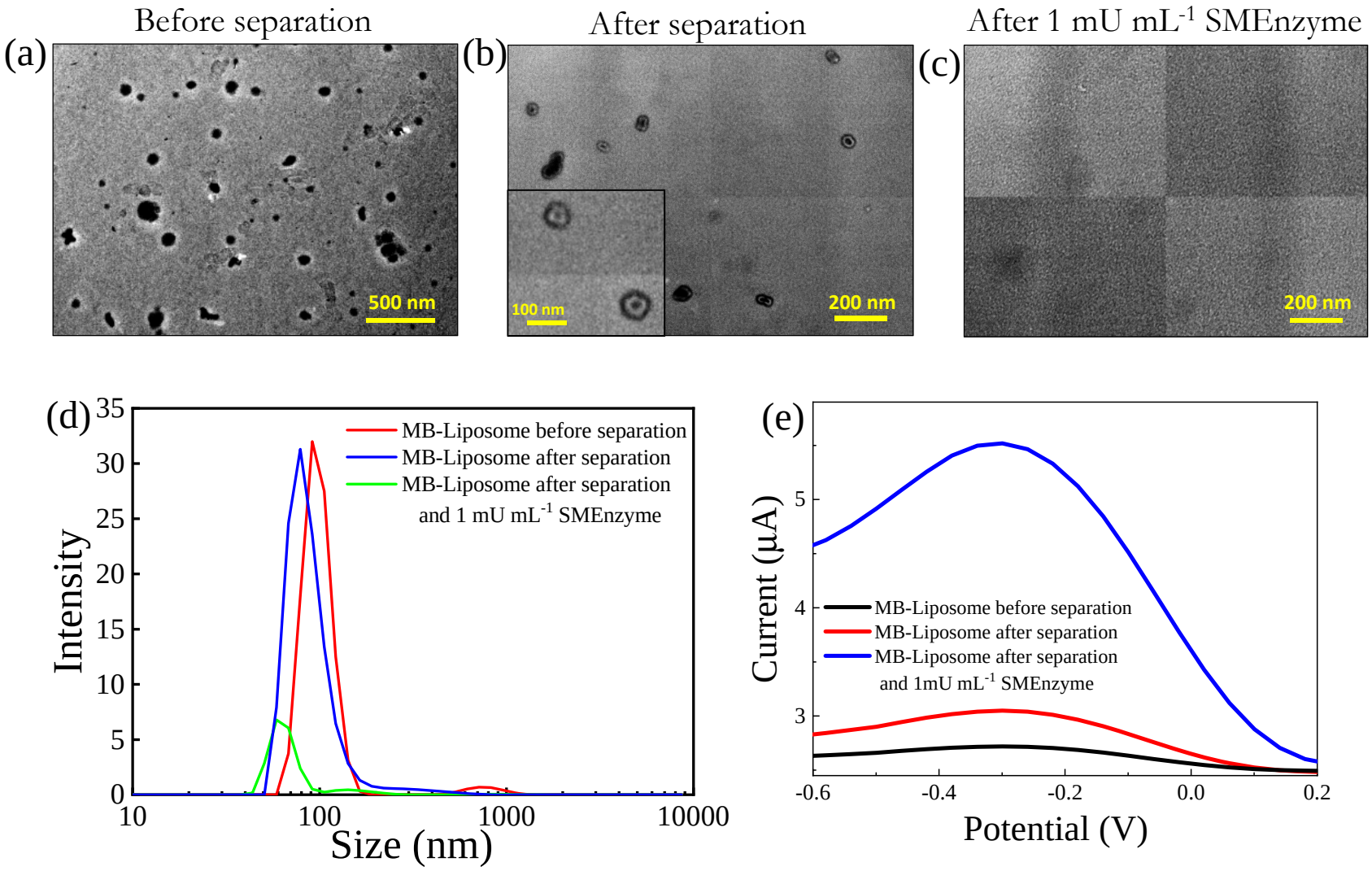
(a)
Before separation
500 nm
(b)
After separation
100 nm
200 nm
(c)
After 1 mU mL-1 SMEnzyme
200 nm
(d)
Intensity
Size (nm)
MB-Liposome before separation
MB-Liposome after separation
MB-Liposome after separation
and 1 mU mL-1 SMEnzyme
(e)
Current (μA)
Potential (V)
MB-Liposome before separation
MB-Liposome after separation
MB-Liposome after separation
and 1mU mL-1 SMEnzyme

Chowdhury et al., Fig. 4

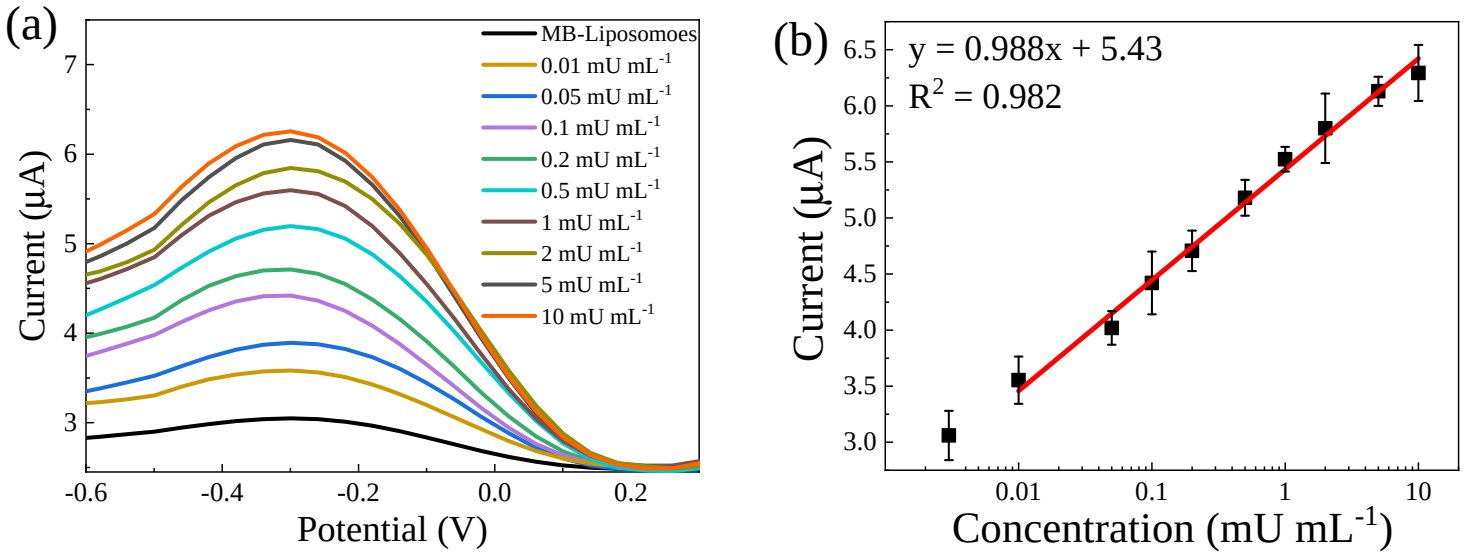

Chowdhury et al., Fig. 5

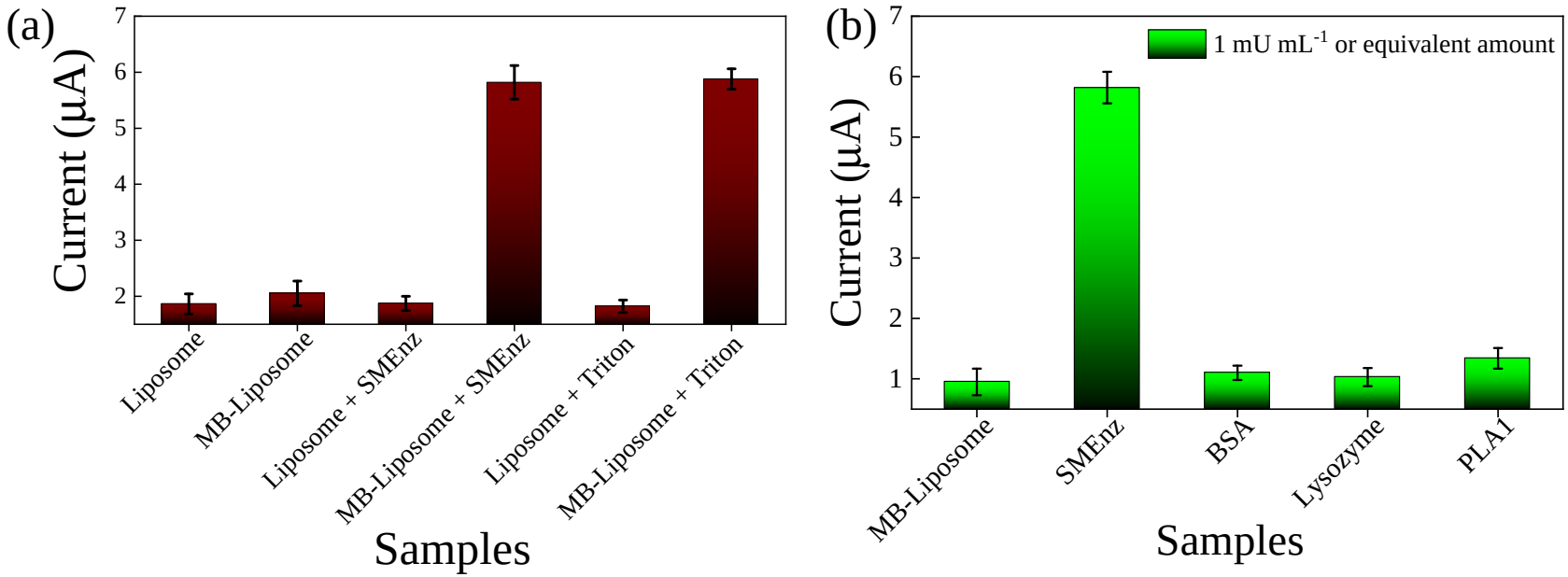

Chowdhury et al., Fig. 6

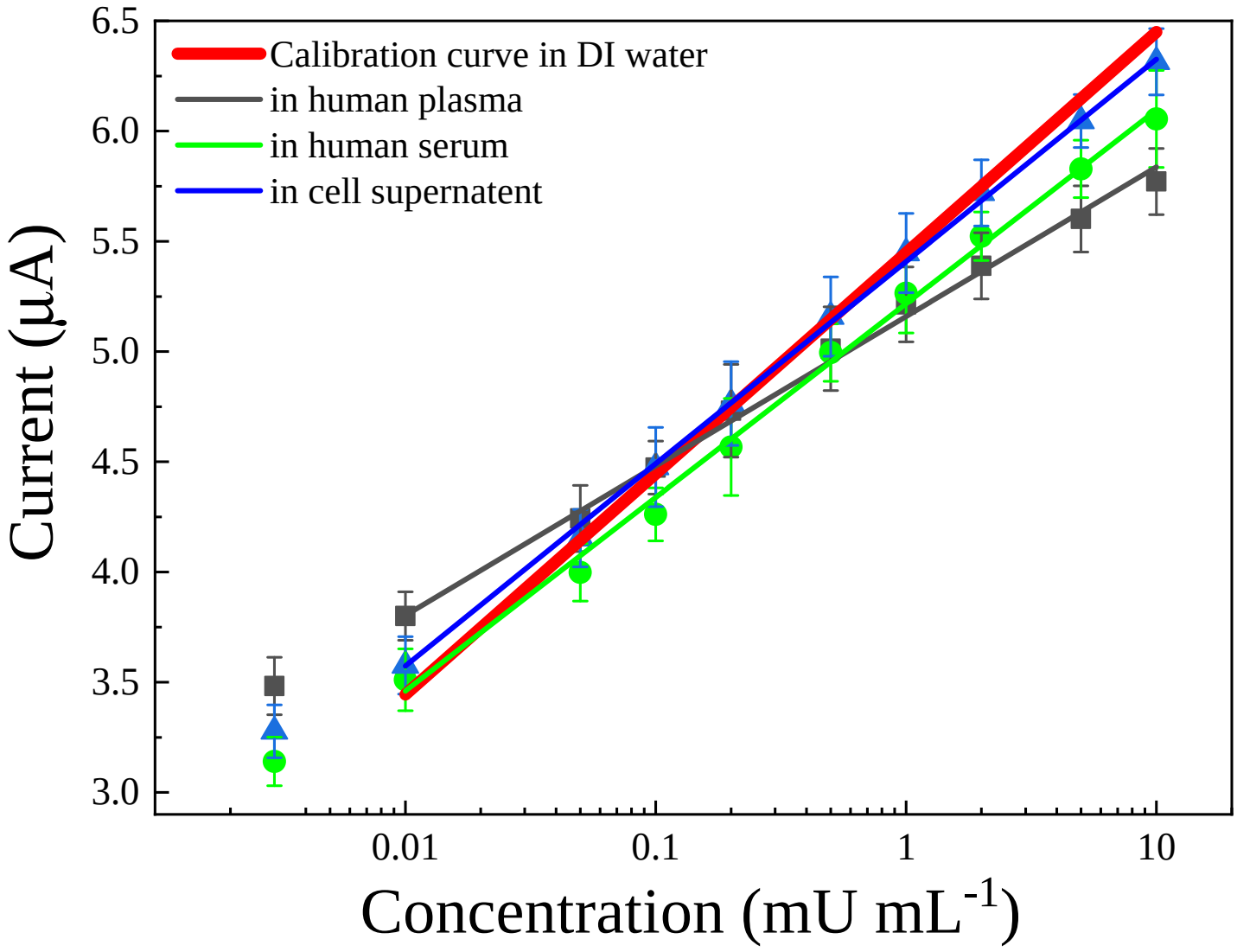

Supplementary Information

Methylene blue-encapsulated liposomal biosensor for electrochemical detection of sphingomyelinase enzyme

Ankan Dutta Chowdhury[a] and Enoch Y. Park[a,b,*]

[a] *Research Institute of Green Science and Technology, Shizuoka University, 836 Ohya Suruga-ku, Shizuoka 422-8529, Japan*

[b] *Department of Bioscience, Graduate School of Science and Technology, Shizuoka University, 836 Ohya Suruga-ku, Shizuoka 422-8529, Japan*

[*]Corresponding Author at Research Institute of Green Science and Technology, Shizuoka University, 836 Ohya Suruga-ku, Shizuoka 422-8529, Japan.

E-mail addresses: park.enoch@shizuoka.ac.jp (E.Y. Park), ankan.dutta.chowdhury@shizuoka.ac.jp (A.D. Chowdhury).

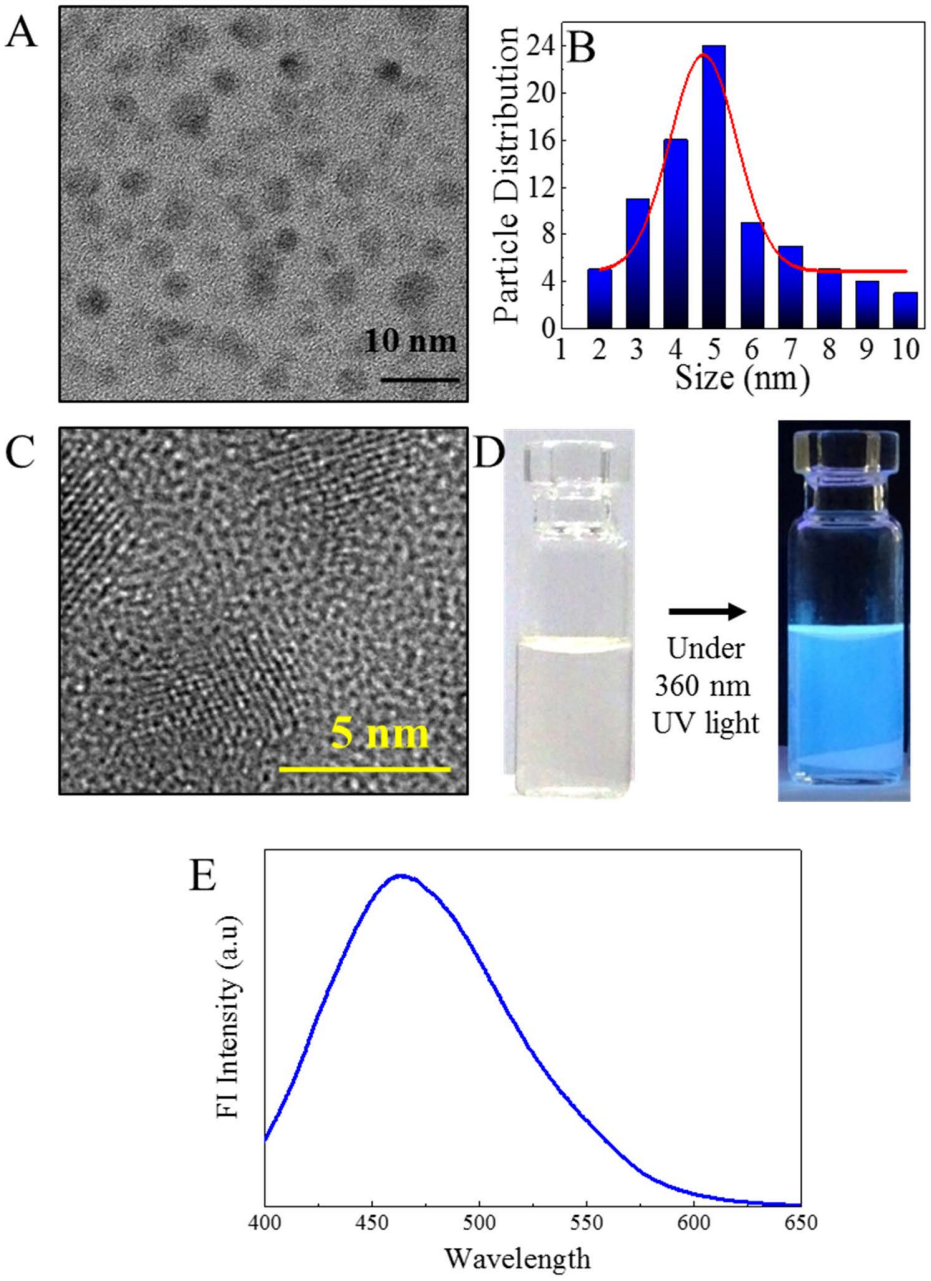

Fig. S1. Characterisations of N,S-GQDs: (A) Homogeneous distributed TEM image and (B) particle size distribution, (C) HRTEM image of a single particle of N,S-GQDs, (D) optical property of N,S-GQDs in visible light and under 360 nm UV-lamp and (E) fluorescence emission at the excitation 360 nm.

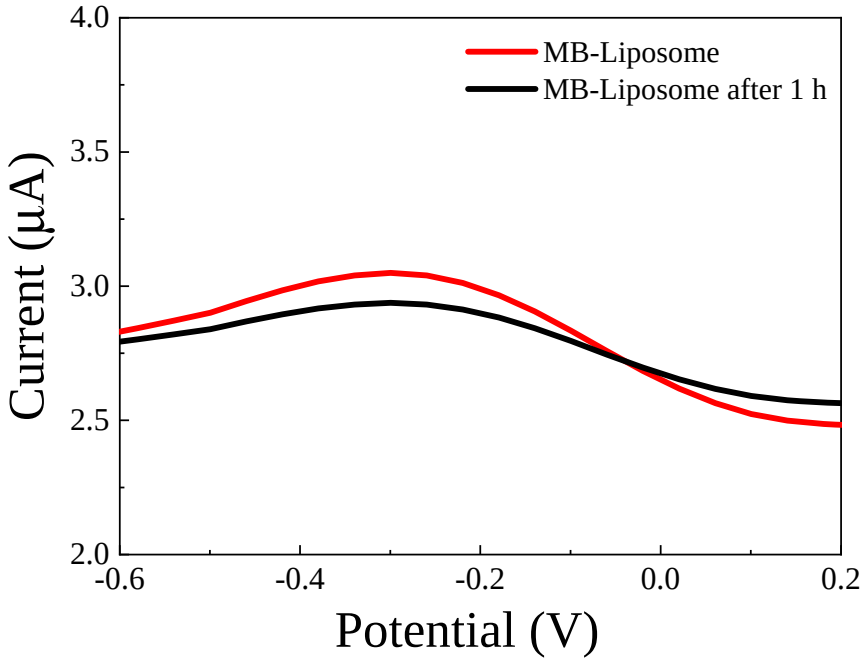

Fig. S2. Stability of Mb-Liposome over a time period of 1 h which is almost unchanged in DPV.